Transcriptomics reveals the mycoparasitic strategy of the mushroom *Entoloma abortivum* on species of the mushroom *Armillaria*

Running title: Mycoparasitism of *Entoloma abortivum*

Rachel A. Koch[1] and Joshua R. Herr[1,2,#]

[1]Department of Plant Pathology, University of Nebraska, Lincoln, NE 68503, USA;

[2]Center for Plant Science Innovation, University of Nebraska, Lincoln, NE 68588, USA;

[#]Correspondence: Joshua R. Herr (jherr@unl.edu)

Abstract word count (including abstract and importance): 363

Text word count: 4938

ABSTRACT

During mycoparasitism, a fungus—the host—is parasitized by another fungus—the mycoparasite . The genetic underpinnings of these relationships have been best characterized in Ascomycete fungi. However, within Basidiomycete fungi, there are rare instances of mushroom-forming species parasitizing the reproductive structures, or sporocarps, of other mushroom-forming species. One of the most enigmatic of these occurs between *Entoloma abortivum* and species of *Armillaria*, where hyphae of *E. abortivum* are hypothesized to disrupt the development of *Armillaria* sporocarps, resulting in the formation of carpophoroids. However, it remains unknown whether carpophoroids are the direct result of a mycoparasitic relationship. To address the nature of this unique interaction, we analyzed gene expression of field-collected *Armillaria* and *E. abortivum* sporocarps and carpophoroids. Transcripts in the carpophoroids are primarily from *E. abortivum*, supporting the hypothesis that this species is parasitizing *Armillaria*. Most notably, we identified differentially expressed *E. abortivum* β-trefoil-type lectins in the carpophoroid, which we hypothesize bind to *Armillaria* cell wall galactomannoproteins, thereby mediating recognition between the mycoparasite and the host. The most significantly upregulated *E. abortivum* transcripts in the carpophoroid code for oxalate decarboxylases—enzymes that degrade oxalic acid. Oxalic acid is a virulence factor in many plant pathogens, including *Armillaria* species, however, *E. abortivum* has evolved a sophisticated strategy to overcome this defense mechanism. The number of gene models and genes that code for carbohydrate-active enzymes in the *E. abortivum* transcriptome were reduced

compared to other closely related species, perhaps as a result of the specialized nature of this interaction.

IMPORTANCE

By studying fungi that parasitize other fungi, we can understand the basic biology of these unique interactions. Studies focused on the genetic mechanisms regulating mycoparasitism between host and parasite have thus far concentrated on a single fungal lineage within the Ascomycota. The work presented here expands our understanding of mycoparasitic relationships to the Basidiomycota, and represents the first transcriptomic study to our knowledge that examines fungal-fungal relationships in their natural setting. The results presented here suggest that even distantly related mycoparasites utilize similar mechanisms to kill their host. Given that species of the mushroom-forming pathogen *Armillaria* cause plant root-rot diseases in many agroecosystems, an enhanced understanding of this interaction may contribute to better control of these diseases through biocontrol applications.

70 **INTRODUCTION**

71 Fungal mycoparasitism is a nutritional strategy where a living fungus—the host—is
72 parasitized by and acts as a nutrient source for another fungus—the mycoparasite.
73 Certain species of fungi in the Hypocreales (Ascomycota) are among the best-studied
74 mycoparasites. Perhaps the most well-known of these are species of *Trichoderma* and
75 *Clonostachys rosea*, which have biocontrol activity against plant pathogenic species of
76 *Botrytis*, *Fusarium*, *Pythium*, and *Rhizoctonia* (1, 2). Other fungal mycoparasites in the
77 Hypocreales include *Tolypocladium* species, many of which are parasites on the
78 reproductive structures, or sporocarps, of species in the genus *Elaphomyces*
79 (Eurotiales, Ascomycota) (3), as well as *Escovopsis weberi*, which is a specialized
80 necrotrophic parasite of fungal gardens of attine ants (4, 5).

81 Less studied examples of mycoparasitism involve mushroom-forming fungi that
82 parasitize other mushroom-forming fungi. Fewer than 20 reported mushroom species
83 are capable of engaging in this type of interaction, making it an incredibly rare
84 phenomenon given the total number of mushroom-forming fungi (6, 7). Examples of this
85 interaction include *Volvariella surrecta*, which fruits from the pileus of its host, *Clitocybe*
86 *nebularis* (8), which appears to remain unaffected by its parasite (7). More commonly,
87 though, mushroom mycoparasites deform host sporocarps and likely prevent the
88 dispersal of their spores. *Pseudoboletus parasiticus* fruits from the sporocarps of
89 *Scleroderma* species, which, after infection, are no longer able to mature and disperse
90 their spores (9). *Psathyrella epimyces* causes the deformation of sporocarp tissue of its
91 host, *Coprinus comatus* (10). Additionally, of the ten mushroom species in the genus

92 *Squamanita*, all are known to be parasites of sporocarps of species in the genera
93 *Cystoderma*, *Galerina*, *Hebeloma*, and *Inocybe* (7).
94 One of the most commonly encountered putative mycoparasitic interactions
95 between two mushrooms involves species of *Armillaria* (Fig. 1A) and *Entoloma*
96 *abortivum* (Fig. 1B). *Entoloma abortivum* is often encountered fruiting in soil, humus, or
97 decaying logs in deciduous woods (11), while *Armillaria* species are facultative
98 necrotrophs that can cause root rot in forest and agronomic systems worldwide (12, 13).
99 Traditionally, *E. abortivum* was thought to exist in two forms: the typical mushroom form,
100 which has a gray stipe, gray pileus and pink gills (Fig. 1B), and the carpophoroid form,
101 which is white, subglobose and lacks well-formed gills (Fig. 1C–D). The carpophoroid
102 form has traditionally been assumed to be *E. abortivum* sporocarps that did not develop
103 properly due to parasitism by *Armillaria* species (11). However, macro- and microscopic
104 studies of carpophoroid field collections determined that carpophoroids actually
105 represent malformed *Armillaria* sporocarps permeated by *E. abortivum* hyphae (14).
106 Laboratory inoculation experiments showed that *E. abortivum* interacts with *Armillaria*
107 sporocarps to disrupt their morphological development (14).
108 Whether carpophoroids are the result of a mycoparasitic relationship, where *E.*
109 *abortivum* serves as the mycoparasite and *Armillaria* species serve as the host, remains
110 unknown. In order to address this, we initiated a transcriptome study after we
111 encountered all three components of this system fruiting in close proximity—
112 carpophoroids and individual sporocarps of *E. abortivum* and *Armillaria*. For a
113 mycoparasite to be successful, there are several crucial steps in the utilization of a
114 fungal host for nutrition. These steps include: 1) sensing the host; 2) recognition and

115 attachment to host hypha; 3) initiating defense responses; and 4) the eventual demise
116 of the host (15). Previous genomic and transcriptomic studies elucidated the genetic
117 machinery that model mycoparasites utilize during each of these steps (15–17). In this
118 work, we used transcriptomic and meta-transcriptomic techniques to analyze the
119 genomic toolbox of *E. abortivum* and *Armillaria* during the carpophoroid stage. We show
120 that the gene expression profiles of *E. abortivum* resemble those of known
121 mycoparasitic species, as well as predict certain genes in both species that facilitate this
122 interaction. Additionally, we used transcriptomic information to determine the species of
123 *Armillaria* involved in this association.
124

125 **RESULTS**

126 ***Transcriptome assemblies of* Entoloma abortivum *and* Armillaria*.*** In order to
127 benchmark gene diversity and baseline expression levels of the field-collected
128 mushroom species in our study, we sequenced the sporocarp transcriptomes of *E.*
129 *abortivum* and the *Armillaria* species found in close proximity to the carpophoroids. To
130 date, there are several transcriptomic studies of *Armillaria* species (18, 19), but none for
131 any *Entoloma* species. The assembled transcriptome of *E. abortivum* was just under
132 120 million base pairs. There were a total of 43,599 contigs and an N50 value of 3,527;
133 94.5% of benchmark universal single-copy orthologs (BUSCOs) from the Agaricales
134 were present in the *E. abortivum* transcriptome. A large number of contigs represented
135 duplicated gene models with potential splice variation. Within the contigs, a total of
136 9,728 unique gene models were recovered in the transcriptome assembly (Fig. 2) with
137 603 genes differentially expressed in the carpophoroid tissue and 403 genes

138 differentially expressed in the sporocarp tissue (Fig. 3). The transcriptome contained
139 195 genes that code for carbohydrate-active enzymes (CAZymes). The transcriptome
140 lacks any genes that code for cellobiohydrolases (GH6 and GH7), xylanases (GH10,
141 GH11, GH30) and auxiliary proteins like polysaccharide monooxygenases (GH61), but
142 does contain nine chitinases (GH18) (Fig. 2). Genes detected in the *E. abortivum*
143 transcriptome that might be important in mycoparasitic interactions include: ten putative
144 secondary metabolite gene clusters, one G-coupled protein receptor (GCPR), 38 ATP-
145 binding cassette (ABC) transporters and 113 genes from the major facilitator
146 superfamily (MFS) (Fig. 3). The average gene expression (in normalized units of
147 trimmed mean of m-values (TMM)) of the ten most highly expressed *E. abortivum* genes
148 in the sporocarp ranged from 4,333 to 17,890. Information about the ten most highly
149 expressed transcripts in the sporocarps is available in Table 1.

150 The assembled transcriptome of *Armillaria* was just over 138 million base pairs.
151 There were a total of 63,905 contigs, an N50 value of 2,845, and 97.8% of the BUSCOs
152 representative of the Agaricales were present in the transcriptome. Again, a large
153 number of the contigs represented duplicated gene models with potential splice
154 variation. A total of 38,215 unique gene models were recovered (Fig. 2) and 2,619
155 transcripts were differentially expressed in the carpophoroid tissue, whereas 9,820 were
156 differentially expressed in the sporocarp tissue (Fig. 3). The transcriptome contained
157 580 genes that code for CAZymes, with 34 of those coding for chitinases (Fig. 2).
158 Genes detected in the *Armillaria* transcriptome that might be important in mycoparasitic
159 interactions include: 12 putative secondary metabolite gene clusters, five GCPRs, 59
160 ABC transporters and 144 MFS transcripts (Fig. 3). The average TMM of the ten most

161 highly expressed *Armillaria* genes in the sporocarp ranged from 8,438 to 36,477. The
162 most highly expressed gene was annotated as a cell wall galactomannoprotein (Fig. 4
163 and 5) (Table 2), while, notably, the fourteenth most highly expressed gene in the
164 sporocarp coded for isocitrate lyase (Table 2, Fig. 5).
165
166 **Metatranscriptomic analysis of combined fungal hyphae in carpophoroid tissue.**
167 We sequenced the metatranscriptome of the mixed tissue in the carpophoroids that are
168 typically found when *E. abortivum* and species of *Armillaria* are found in close proximity.
169 In the carpophoroid tissue, significantly more transcriptomic reads from *E. abortivum*
170 were identified than from *Armillaria* sp. ($t_{(8)} = 16.6$, $p = 1.77\times10^{-7}$, $n = 9$ replicates per
171 species) (Fig. 6). The average number of *E. abortivum* mapped reads in the
172 carpophoroid tissue was 2,613,988, while the average number of *Armillaria* mapped
173 reads was 74,880 (Fig. 6). Multidimensional scaling (MDS) plots of *E. abortivum* (Fig.
174 7A) and *Armillaria* (Fig. 7B) show that the genetic distance between the *E. abortivum*
175 sporocarps and the carpophoroid is less than the distance between *Armillaria*
176 sporocarps and the carpophoroid.
177 The average TMM of the top ten most highly expressed *E. abortivum* genes in
178 the carpophoroid ranged from 9,075 to 68,720 (Table 1), while the average TMM of the
179 top ten most highly expressed *Armillaria* transcripts in the carpophoroid ranged from
180 300 to 9,049 (Table 2). The first and third most highly expressed *E. abortivum*
181 transcripts in the carpophoroid tissue code for two oxalate decarboxylases, both of
182 which were significantly differentially expressed in the carpophoroid tissue compared to
183 the sporocarp (Figs. 3, 4, 5 and Table 1). There were other differentially expressed *E.*

184 *abortivum* transcripts in the carpophoroid that were not as highly expressed that may
185 also play a role in mycoparasitism. These include three β-trefoil-type lectins, three ABC
186 transporters, two chitinases, and 14 MFS transcripts (Fig. 3, Table 1). No transcripts
187 involved in secondary metabolite gene clusters were differentially expressed in the
188 carpophoroids (Fig. 3). Opposingly, two *Armillaria* transcripts that code for putative
189 senescence-associated proteins were significantly expressed in the carpophoroid
190 compared to the sporocarp as well as a heat shock protein (Table 2).
191
192 ***Phylogenetic placement of* Armillaria *reads.*** Phylogenomic analysis of 100
193 randomly-selected *Armillaria* BUSCOs generated in this study, in conjunction with
194 previously published *Armillaria* genomes, shows a strongly supported sister relationship
195 with an *A. mellea* specimen from France (100% BS) (Fig. 8A). Phylogenetic analysis of
196 all ITS sequences characterized as *A. mellea* from GenBank shows that this specimen
197 is conspecific with specimens from eastern North American (Fig. 8B).
198
199 **DISCUSSION**
200 The formation of carpophoroids associated with species of *E*. *abortivum* have
201 traditionally been thought to be the result of an *Armillaria* species attacking and
202 parasitizing *Entoloma* sporocarps (11), a conclusion drawn based on the fact that
203 *Armillaria* species are wide-spread forest pathogens (12). However, subsequent studies
204 have shown the opposite: the production of carpophoroids are the result of *E. abortivum*
205 disrupting the development of *Armillaria* sporocarps (14). Here, we employed RNA
206 sequencing and differential gene expression analysis on field-collected fungal tissue of

207 each of the three components of this association to better understand the mechanistic
208 basis of this interaction. We determined that *E. abortivum* reads in the
209 metatranscriptome of the carpophoroid tissue—which can be interpreted as a measure
210 of living tissue—are almost 35 times more abundant in the carpophoroid tissue
211 compared to *A. mellea* reads (Fig. 6). This finding suggests that carpophoroids are
212 structures that result from *E. abortivum* parasitizing, and eventually killing, its *Armillaria*
213 host under natural conditions. Additionally, the genetic differences between
214 carpophoroids and sporocarps is much smaller for *E. abortivum* than for *Armillaria* (Figs.
215 3, 4, and 7) , which could be suggestive that mycoparasitism is part of the life history of
216 *E. abortivum* and fewer genetic shifts are necessary to transition between the
217 carpophoroid and sporocarp.
218 Fungal-fungal necrotrophic mycoparasitic interactions are multistage processes
219 that are best studied in model species, such as those in the genera *Trichoderma*,
220 *Coniothyrium, Clonostachys* and *Tolypocladium* (17). Genomic and transcriptomic
221 studies of necrotrophic mycoparasites show a convergence of significant genetic
222 mechanisms at each stage (17). The *E. abortivum* genes that are upregulated with
223 statistical significance in the carpophoroid tissue are largely consistent with other
224 examples of necrotrophic mycoparasites in the Ascomycota. In the carpophoroid tissues
225 we analyzed, *E. abortivum* appears to employ much of its energy on recognition and
226 defense responses (Fig. 5). Inversely, the *Armillaria* sporocarps we analyzed illuminate
227 possible mechanisms by which these two species recognize one another and how
228 *Armillaria* responds to parasitism (Fig. 5).
229

230 ***The genetics of the* Entoloma-Armillaria *mycoparasitic interaction.*** A crucial step in
231 a successful mycoparasite's life history is the ability to sense its host. Genes involved in
232 the recognition of the fungal prey include those that code for GPCRs (15, 17). However,
233 we did not find any of these genes that were differentially expressed by *E. abortivum* in
234 the carpophoroid tissue (Fig. 3). Given the significantly fewer number of *Armillaria* reads
235 in the carpophoroid tissue compared to *E. abortivum*, we presume that these
236 carpophoroids are relatively advanced in age, and expression of the genes used for
237 sensing the presence of the host are no longer necessary.

238 We also identified three *E. abortivum* genes that code for β-trefoil-type lectins—
239 proteins that bind to galactose units of sugar chains (20)—that were significantly
240 upregulated in the carpophoroid tissue (Figs. 3 and 5). In *Trichoderma* species, the
241 recognition, attachment, and coiling around a fungal substrate is dependent on the
242 recognition of lectins expressed by the fungal host (21, 22). Interestingly, the most
243 abundant and differentially expressed gene produced in the *Armillaria* sporocarps, the
244 substrate to which *E. abortivum* hyphae attach, codes for a cell wall
245 galactomannoprotein (Figs. 4 and 5). These proteins belong to a group of
246 polysaccharides which consist of a mannose backbone with galactose side chains, and
247 are known to make up a major part of the cell wall of some fungal species (23). This
248 particular galactomannoprotein appears to be specific to *Armillaria* species. Watling (11)
249 commented on the highly specific nature of this interaction and that it has only been
250 documented occurring between *E. abortivum* and *Armillaria* species. One possible
251 mediator of the specificity of this interaction could be the galactose sugars on the
252 mannose protein (only known thus far from *Armillaria* species) are the means by which

253 *E. abortivum* β-trefoil-type lectins recognize and attach to its *Armillaria* host. However,
254 more genome sequencing of other Agaricales species is needed to determine whether
255 this protein is truly specific to species in the genus *Armillaria*.

256 During mycoparasitic interactions, the fungal host responds by mounting its own
257 defense, and a successful mycoparasite must be able to cope with this counterattack
258 (15, 17). Two of the most abundant and significantly upregulated *E. abortivum* genes in
259 the carpophoroid tissue code for oxalate decarboxylases—enzymes responsible for the
260 degradation of oxalic acid (OA) (Figs. 3, 4, 5D, Table 1). In at least one known well-
261 studied mycoparasitic interaction, OA is secreted by the fungal host, *Sclerotinia*
262 *sclerotiorum*, in reaction to penetration by its mycoparasite, *Coniothyrium minitans*. The
263 acidic environment created by the secreted OA inhibits conidial germination and
264 suppresses mycelial growth of *C. minitans* (24). However, *C. minitans* nullifies the
265 growth-suppressing effects of OA or OA-mediated low pH by degrading the OA (25, 26),
266 an enzymatic process largely mediated by oxalate decarboxylase. Because of this,
267 oxalate decarboxylase plays an imperative role in mycoparasitism as OA degradation is
268 vital for infection of the fungal host (27).

269 The secretion of OA is also a broader defense mechanism employed by some
270 plant pathogens to compromise the defense responses of the host plant by creating an
271 acidic environment (28). One of the components of the plant-parasitic arsenal of
272 *Armillaria* species may be the production of OA (29). One differentially upregulated
273 gene in *Armillaria* sporocarps is isocitrate lyase (Fig. 5), which is involved with OA
274 biosynthesis in other fungal pathogens (30, 31). We have two hypotheses for the
275 upregulation of isocitrate lyase in the apparently asymptomatic *Armillaria* sporocarp

276 tissue. An explanation might be that isocitrate lyase is more upregulated in situations
277 where *Armillaria* is in contact with a plant host and OA biosynthesis is high. One might
278 also suggest that *Armillaria* is monitoring the close proximity of *E. abortivum* and it is
279 preemptively launching a defense before hyphal contact is made. However, the
280 upregulation of oxalate decarboxylases by *E. abortivum* suggests it has evolved a
281 sophisticated strategy to inactivate the potentially lethal defenses of *Armillaria* exhibited
282 by the subsequent downregulation of isocitrate lyase in the carpophoroid tissue (Fig. 5).
283 Other ways that mycoparasites cope with the counterattack launched by their
284 host include actively extruding host-secreted toxins. Here, we hypothesize that active
285 extrusion of toxins secreted by the host occurs in the *E. abortivum* carpophoroid tissue
286 via membrane transporters in the ABC superfamily (32–34). Three ABC transporters
287 were differentially expressed in the carpophoroid tissue (Fig. 3). Another group of genes
288 that were differentially expressed by *E. abortivum* in the carpophoroid belong to the
289 major facilitator superfamily (MFS) transporters (Fig. 3). In *C. rosea*, there was selection
290 for genes in this family that were related to drug resistance, and the transport of
291 secondary metabolites, small organic compounds and carbohydrates (35). Their
292 importance to mycoparasitism in *C. rosea* is predicted to invoke efflux-mediated
293 protection against exogenous or endogenous secondary metabolites and nutrient
294 uptake (35). MFS transporters have also been shown to be induced in other
295 mycoparasitic species (16, 36), but their exact biological roles have not been
296 investigated.
297 In mycoparasitism, the final death of the host often results from the synergistic
298 actions of cell wall-hydrolytic enzymes and antifungal secondary metabolites (15, 17).

299 No secondary metabolite gene clusters identified in the *E. abortivum* transcriptome were
300 significantly upregulated in the carpophoroid tissue (Fig. 3). In some mycoparasitic
301 relationships, the secretion of secondary metabolites occurs early on in the interaction,
302 including in *E. weberi*, which secretes toxic compounds that kill the leafcutter ant garden
303 before contact (5). In culture experiments between *Armillaria* isolates and *E. abortivum*,
304 the growth of *Armillaria* was severely inhibited by the presence of *E. abortivum* (37).
305 This suggests that *E. abortivum* may potentially secrete a toxic compound early in the
306 interaction that inhibits the growth of *Armillaria*. Given that significantly more of the living
307 tissue in the carpophoroids belonged to *E. abortivum* (Fig. 6), it is possible that much of
308 the *Armillaria* tissue was killed preceding the full development of the carpophoroid.
309 We hypothesize that the upregulated β-trefoil-type lectin in *E. abortivum* that may
310 be important in hyphal recognition may also be cytotoxic towards *Armillaria*. This type of
311 lectin has sequence homology, as well as putative structural similarity, to the B-subunit
312 of ricin, a toxic protein from the castor bean *Ricinus communis* (38). An array of β-
313 trefoil-type lectins have been characterized from the sporocarps of the mushroom-
314 forming species *Clitocybe nebularis* (39), *Coprinus cinerea* (40), *Macrolepiota procera*
315 (41) and *Boletus edulis* (42). These mushroom lectins exhibit entomotoxic activity (43)
316 as well as nematoxic activity (40, 41, 44). Taken together, it is possible that these *E.*
317 *abortivum* β-trefoil-type lectins may also function as toxins towards *Armillaria*. While the
318 *E. abortivum* genes coding for these lectins are not in the highest abundance in the
319 carpophoroid tissue (Fig. 5), this could be because most of the *Armillaria* sporocarp
320 tissue is already dead and the potential lethal effects of these genes are no longer
321 necessary.

322 Chitin is an essential polymer in fungal cell walls (45) and is an important target
323 during mycoparasitic attack (17). Indicative of the importance of chitinases in
324 mycoparasitic interactions, members of the genus *Trichoderma*, as well as *T.*
325 *ophioglossoides* and *E. weberi,* have an increased number of genes coding for the
326 glycoside hydrolase family 18 (16, 46–49). Nine fungal chitinases were detected in the
327 transcriptome of *E. abortivum*, although only two were differentially expressed in the
328 carpophoroid tissue (Fig. 3) and were not abundant in comparison to other genes,
329 suggesting minimal significance at this stage in carpophoroid development. One
330 possibility for this difference in abundance could be the result of the putatively acidic pH
331 in the carpophoroid that we infer based on the high gene expression of oxalate
332 decarboxylases. In *C. minitans*, chitinase activity is positively correlated with ambient
333 pH ranging from three to eight (50), so it is possible that chitinase activity in *E.*
334 *abortivum* will increase after a neutral pH is restored.
335 Some of the putatively mycoparasitism-related genes outlined above were also
336 differentially expressed by *Armillaria* in the carpophoroid tissue. These include genes
337 that code for MFS, ABC transporters, chitinases, and secondary metabolite gene
338 clusters (Fig. 3). This suggests that *Armillaria* may be using many of the same genetic
339 mechanisms to defend itself against parasitism by *E. abortivum*. Additionally, the degree
340 of expression changes—both in the number of differentially expressed genes and the
341 log-fold change (logFC)—between the sporocarp and carpophoroid is much greater in
342 *Armillaria* compared to *E. abortivum* (Fig. 3, 4, 7), which could be a reflection of the
343 level of defense *Armillaria* is mounting. However, this defense is apparently not enough
344 to overcome the parasitic adaptations of *E. abortivum*.

345

346 ***Gene and CAZyme content of* E. abortivum*.*** The number of predicted gene models in
347 the transcriptome of *E. abortivum* was 9,728, which is markedly fewer than the number
348 of gene models in the genomes of its closest sequenced relatives (Fig. 2B). Additionally,
349 relative to other closely related mushroom species, *E. abortivum* also exhibits a strong
350 reduction in several gene families encoding CAZymes (Fig. 2C), and contains no
351 cellobiohydrolases, xylanases, or polysaccharide monooxygenases. This is similar to *E.*
352 *weberi*, which also has a reduced genome and CAZyme repertoire—hypothesized to be
353 the result of its highly specialized interaction with leafcutter ant gardens (46). Therefore,
354 it is possible that *E. abortivum* only retained the CAZymes and accessory genes
355 necessary to interact with *Armillaria* species. While a genome sequence of *E. abortivum*
356 will be necessary to confirm this reduction, the BUSCO analysis verified that the *E.*
357 *abortivum* transcriptome contains nearly 95% of the core set of eukaryotic genes.
358 Another possibility for the reduction in CAZymes could be explained by a broader
359 nutritional strategy employed by *Entoloma* species, some of which form ectomycorrhiza-
360 like structures on host plant species (51–53). Ectomycorrhizal species have a marked
361 reduction in CAZymes in comparison to their saprotrophic ancestors (54), which we also
362 observe with *Tricholoma matsutake* (Fig. 2C). However, microscopic analyses of
363 *Entoloma* ectomycorrhizae-like structures suggest that some species destroy root
364 meristems and young root cells, suggestive of a more parasitic relationship (51, 52).
365 One explanation is that *Entoloma* species are actually parasites of true
366 ectomycorrhizae. This explanation would also add credence to the evidence that
367 *Entoloma* species are difficult to culture and are slow growing (53). Additional research

368 to understand the nutritional strategy employed by this lineage will inform us as to
369 whether fungal parasitism in this group is more common than it is currently understood
370 to be.
371
372 ***Identity of* Armillaria *species in this interaction.*** Phylogenomic analysis of the
373 *Armillaria* transcripts generated in this study suggest that the *Armillaria* species
374 parasitized in this particular relationship is sister to an *A. mellea* specimen collected
375 from western Europe (Fig. 8A). An ITS-based phylogenetic analysis shows the
376 *Armillaria* specimen collected in this study is conspecific with other *A. mellea* collections
377 from eastern North America (Fig. 8B). *Armillaria mellea* has previously been identified
378 as a host of *E. abortivum* (11, 14), but this interaction does not appear specific to just *A.*
379 *mellea*. Interestingly, *Armillaria* species parasitized by *E. abortivum* appear to be only
380 those present in Eastern North America and Asia (14, 37, 55).
381
382 ***Conclusions.*** Data from this study support the hypothesis that *E. abortivum* is a
383 mycoparasite of *Armillaria* sporocarps. Three β-trefoil-type lectins are differentially
384 expressed by *E. abortivum* in the carpophoroid tissue, and we propose that these
385 lectins mediate recognition with *Armillaria* sporocarps through binding to an *Armillaria*-
386 specific galactomannoprotein. Additionally, through the use of oxalate decarboxylase, *E.*
387 *abortivum* is likely defending against the secretion of OA by *Armillaria*. These strategies
388 employed by *E*. *abortivum* for recognition and defense are similar to mechanisms
389 utilized by other mycoparasites, suggesting that even distantly related mycoparasites
390 utilize similar genetic mechanisms to mediate mycoparasitic interactions. While we were

391 able to speculate about what is occurring during other stages of mycoparasitism (i.e.
392 sensing the host and killing and consuming the host), future studies using both culture
393 methods and metatranscriptomics of naturally collected carpophoroids at different life
394 stages (i.e. younger and older specimens) will be necessary to completely tease apart
395 the mycoparasitic strategies employed by *E. abortivum*.
396

397 **MATERIALS AND METHODS**

398 **Sample collection, preparation, and sequencing.** Sporocarps of *Armillaria* sp., *E.*
399 *arbotivum*, and the mixed-tissue carpophoroids were observed fruiting in proximity to
400 one another on 18 September 2015 within the Baker Woodlot and Rajendra Neotropical
401 Migrant Bird Sanctuary, Michigan State University, East Lansing, MI 48823 (42°42'56.4"
402 N, 84°28'34.4" W) (collection accession: JRH 2446). Entire sporocarps were collected
403 and immediately flash frozen in liquid nitrogen and subsequently stored at -80°C. At the
404 time of processing, three biological replicates of each of the three tissue types
405 (*Armillaria sp*. sporocarp, *E. abortivum* sporocarp, and carpophoroid), were individually
406 ground in liquid N_2. Total RNA was then extracted from the ground tissue using the
407 Qiagen RNeasy kit (Qiagen Inc., Hilden, Germany) according to manufacturer's
408 protocol. RNA concentration and quality for each of the samples were assessed on a
409 DeNovix DS-11 FX Spectrophotometer (DeNovix Inc., Wilmington, DE 19810, USA) and
410 then shipped directly to the University of Minnesota's Genomics Center
411 (https://genomics.umn.edu). Three technical replicates were sequenced for each
412 biological replicate. Transcriptomic and metatranscriptomic libraries were constructed
413 with the TruSeq Standard Total RNA Library Preparation Kit with Ribo-Zero ribosomal

414 reduction following the protocol developed by Schuierer et al. (56). Nucleotide
415 sequencing was performed on the Illumina HiSeq 2500 System (Illumina Inc., San
416 Diego, USA) and paired-end RNA sequence reads of 51 bp were generated for further
417 analysis.
418
419 ***De novo transcriptome assembly, transcript abundance estimation and gene***
420 ***expression analysis.*** The quality of the raw reads was assessed using FastQC version
421 0.11.9 (https://www.bioinformatics.babraham.ac.uk/projects/fastqc). The range of the
422 number of reads for each condition are as follows: *E. abortivum* sporocarps ranged from
423 10,584,302 to 14,473,328; *Armillaria* sporocarps ranged from 11,712,320 to 12,431,979;
424 and the carpophoroids ranged from 9,146,682 to 12,852,086. Sequencing adaptors
425 were trimmed and contaminants filtered for each sample using bbduk
426 (https://jgi.doe.gov/data-and-tools/bbtools/bb-tools-user-guide/bbduk-guide/). Prior to
427 transcriptome assembly, *k-mer* hash sizes were estimated with *khmer* (57). De novo
428 assemblies were constructed independently for both *Armillaria* sp. and *E. arbotivum*
429 with Trinity version 2.11.0 (58) using the trimmed reads generated from the respective
430 sporocarp reads. Assembly statistics for both transcriptomes were generated with
431 QUAST version 5 (59) and transcriptome completeness was assessed by determining
432 the percentage of sequenced BUSCOs in each (60).
433 The results of the *de novo* transcriptome assemblies were used as references to
434 perform sample-specific expression analysis. The trimmed mushroom reads from each
435 of the nine replicates were mapped against their respective reference transcriptomes
436 using Bowtie2 (61) followed by calculation of abundance estimates using RSEM (62).

437 The trimmed carpophoroid reads were also subsequently mapped, following the same
438 protocol as described above, to both the *Armillaria* sp. and *E. arbotivum* transcriptomes.
439 Because of the close phylogenetic relatedness between these two species, and to filter
440 out poorly aligned reads, we only retained mapped reads for all samples that had a
441 MAPQ value of 30 and above, which is equivalent to reads that have a 99.9% chance of
442 hitting the correct match. The R package edgeR (63) and TMM normalization (64) were
443 used to determine differentially expressed transcripts between: 1) *Armillaria* sporocarps
444 and carpophoroids, and 2) *E. abortivum* sporocarps and carpophoroids. Genes were
445 considered differentially expressed if they had a logFC of two or greater and an FDR-
446 adjusted *p*-value, or *q*-value, of < 0.05. All statistical analyses for the packages listed
447 above were conducted using R version 4.0.3 (http://www.r-project.org/).
448 We used SAMtools (65) to determine the number of reads from the
449 carpophoroids that mapped to our reference transcriptomes of *E. abortivum* and our
450 particular *Armillaria* species. To understand whether the number of reads that mapped
451 to the carpophoroids differed significantly between each fungal species, we performed
452 an *F*-test of equality of variances, and then a two-tailed *t*-test assuming unequal
453 variance with a *p*-value < 0.05 denoting significance.
454
455 ***Sporocarp Transcriptome and Carpophoroid Metatranscriptome Annotation.*** We
456 annotated the *Armillaria* sp. and *E. abortivum* transcriptomes using Trinotate version 3.2
457 (66). Briefly, the transcripts were translated to coding protein sequences using
458 TransDecoder version 5.5.0 (http://transdecoder.github.io) following identification of the
459 longest open reading frames. To identify the most likely homologous sequence data, we

460 used *blastx* on the transcripts and *blastp* on the predicted protein sequences (67). Using
461 the predicted protein sequences, we also ran a HMMER (68) search against the PFAM
462 database (69) to identify conserved domains that might be suggestive of function. We
463 also compared these results to currently curated annotation databases such as Gene
464 Ontology (GO) (70) and Kyoto Encyclopedia of Genes and Genomes (KEGG) (71–73).
465 Additionally, we used dbCAN2 (74) to annotate the CAZymes present in both species
466 and compared their CAZy content to other closely related Agaricales species (19, 75–
467 77). Finally, we used antiSMASH version 5.0 (78) to identify transcripts that belong to
468 secondary metabolite gene clusters for both *Armillaria* and *E. abortivum*.
469
470 ***Phylogenetic analysis of* Armillaria *transcripts.*** In order to identify the specific
471 species of *Armillaria* associated in this relationship, we identified BUSCOs (60) from the
472 transcriptome of our *Armillaria* sporocarps along with other *Armillaria* and
473 Physalacriaceae species with previously sequenced genomes (19; 79–81). We
474 randomly selected 100 BUSCOs to reconstruct a phylogenomic tree from the six
475 *Armillaria* specimens (19, 79), *Guyanagaster necrorhizus* (81) and *Cylindrobasidium*
476 *torrendii* (80), which served as the outgroup. Protein-coding sequences were aligned
477 using MAFFT version 7 (82) and non-informative sites and non-aligning regions were
478 trimmed with Gblocks (83). The 100 BUSCOs were concatenated into a supermatrix
479 with 64,436 sites. This supermatrix was used to infer a species tree and branch support
480 using RAxML-NG (84), using a partitioned WAG+G model, where each data partition
481 represented an individual BUSCO.

To supplement the small number of *Armillaria* species with sequenced genomes, we also extracted the internal transcribed spacer (ITS) region from our *Armillaria* transcriptome, including the regions 18S, ITS1, 5.8S, ITS2, and 28S, using ITSx (85). Given the close relationship of our *Armillaria* species to *A. mellea*, we pulled all *A. mellea* ITS sequences from GenBank that included associated location metadata (86–100) (Table S1). These sequences were aligned using MAFFT version 7 (82), with refinements to the alignment performed manually. RAxML-NG (84) was used to reconstruct this phylogeny. Taxa used to root this phylogeny included *A. gemina*, *A. sinapina*, *A. puiggarii* and *A. luteobubalina*—all members of the sister lineage to *A. mellea fide* (13).

Data and code availability. The raw reads generated during this study have been deposited in the NCBI Sequence Read Archive under the BioProject PRJNAXXXXX, while the assembled transcriptomes have been deposited in the NCBI Transcriptome Shotgun Assembly Sequencing Database under the records XXXXXXXXX and XXXXXXXX. All other associated data and code are available at https://github.com/HerrLab/Koch_Arm-Ento_2021.

Acknowledgements

We would like to give special thanks to Andrew Loyd and Eva Skific for providing photos and to Greg Bonito at Michigan State University and his trusty -80°C freezer for generously storing sporocarp and carpophoroid tissue until we were able to transport the tissue to our laboratory. We also want to thank the anonymous reviewers who

provided feedback and comments on the initial submission of this manuscript. This work was completed using the Holland Computing Center of the University of Nebraska, which receives support from the Nebraska Research Initiative. This research was directly supported by start-up funding from the University of Nebraska Agricultural Research Division and the University of Nebraska Office of Research and Economic Development. Additionally, JRH acknowledges funding from the US National Air & Space Administration (Grant #80NSSC17K0737), the US National Science Foundation (EPSCoR Grant #1557417), and US National Institute of Justice (Grant #2017-IJ-CX-0025), all of which indirectly supported this research through the support of research in his laboratory. All of the funding agencies had no role in study design, data collection and interpretation, or the decision to submit the work for publication.

Conflict of Interest Statement

On behalf of all authors, the corresponding author states that there is no conflict of interest.

Author Contributions

JRH initiated the work and sampled field collections; RAK extracted RNA from all the tissue samples and performed all the laboratory work; RAK and JRH performed the experiments, processed the experimental data, analyzed the data, designed the figures, and drafted the manuscript.

528 **REFERENCES**

529 1. Zeilinger S, Omann M. 2007. *Trichoderma* biocontrol: signal transduction
530 pathways involved in host sensing and mycoparasitism. *Gene Regul Syst Bio*
531 **1**:227–234.
532 2. Sun Z-B, Li S-D, Ren Q, Xu J-L, Lu X, Sun M-H. 2020. Biology and applications
533 of *Clonostachys rosea*. *J Appl Microbiol* **129**:486–495.
534 3. Quandt CA, Kepler RM, Gams W, Araújo JPM, Ban S, Evans HC, Hughes D,
535 Humber R, Hywel-Jones N, Li Z, Luangsa-Ard JJ, Rehner SA, Sanjuan T, Sato
536 H, Shrestha B, Sung G-H, Yao Y-J, Zare R, Spatafora JW. 2014. Phylogenetic-
537 based nomenclatural proposals for Ophiocordycipitaceae (Hypocreales) with new
538 combinations in *Tolypocladium*. *IMA Fungus* **5**:121–134.
539 4. Currie CR, Mueller UG, Malloch D. 1999. The agricultural pathology of ant fungus
540 gardens. *Proc Natl Acad Sci U S A* **96**:7998–8002.
541 5. Reynolds HT, Currie CR. 2004. Pathogenicity of *Escovopsis weberi*: the parasite
542 of the attine ant-microbe symbiosis directly consumes the ant-cultivated fungus.
543 *Mycologia* **96**:955–959.
544 6. Redhead SA, Ammirati JF, Walker GR, Norvell LL, Puccio MB. 1994.
545 *Squamanita contortipes*, the Rosetta Stone of a mycoparasitic agaric genus. *Can*
546 *J Bot* **72**:1814–1828.
547 7. Griffith GW, Piotr Gajda K, Detheridge AP, Douglas B, Bingham J, Turner A,
548 Bowmaker V, Evans DA, McAdoo WG, Dentinger BTM. 2019. Strangler
549 unmasked: Parasitism of *Cystoderma amianthinum* by *Squamanita paradoxa* and
550 *S. pearsonii*. *Fungal Ecol* **39**:131–141.

551 8. Weber R, Webster J. 1996. *Volvariella surrecta*: An uncommon mycoparasite.
552 *Mycologist* **10**:160.
553 9. Both EE. 2006. Personal encounters with the parasitic bolete. *Field Mycol* **7**:1–7.
554 10. Buller A. 1924. *Researches on Fungi.* Longmans, London, UK.
555 11. Watling R. 1974. Dimorphism in *Entoloma abortivum*. *Bull Soc Linn Lyon, Num*
556 *Spec* **43**:449–470.
557 12. Baumgartner K, Coetzee MPA, Hoffmeister D. 2011. Secrets of the subterranean
558 pathosystem of *Armillaria*. *Mol Plant Pathol* **12**:515–534.
559 13. Koch RA, Wilson AW, Séné O, Henkel TW, Aime MC. 2018. Resolved phylogeny
560 and biogeography of the root pathogen *Armillaria* and its gasteroid relative,
561 *Guyanagaster*. *BMC Evol Biol* **17**:33.
562 14. Lindner Czederpiltz DL, Volk TJ, Burdsall HH, Jr. 2001. Field observations and
563 inoculation experiments to determine the nature of the carpophoroids associated
564 with *Entoloma abortivum* and *Armillaria*. *Mycologia* **93**:841–851.
565 15. Druzhinina IS, Seidl-Seiboth V, Herrera-Estrella A, Horwitz BA, Kenerley CM,
566 Monte E, Mukherjee PK, Zeilinger S, Grigoriev IV, Kubicek CP. 2011.
567 Trichoderma: the genomics of opportunistic success. *Nat Rev Microbiol* **9**:749–
568 759.
569 16. Quandt CA, Di Y, Elser J, Jaiswal P, Spatafora JW. 2016. Differential expression
570 of genes involved in host recognition, attachment, and degradation in the
571 mycoparasite Tolypocladium ophioglossoides. *G3* **6**:731–741.
572 17. Karlsson M, Atanasova L, Jensen DF, Zeilinger S. 2017. Necrotrophic
573 mycoparasites and their genomes. *Microbiol Spectr* **5**:FUNK-0016-2016.

574 18. Ross-Davis AL, Stewart JE, Hanna JW, Kim MS, Knaus BJ, Cronn R, Rai H,
575 Richardson BA, McDonald GI, Klopfenstein NB. 2013. Transcriptome of an
576 *Armillaria* root disease pathogen reveals candidate genes involved in host
577 substrate utilization at the host–pathogen interface. *For Pathol* **43**:468–477.
578 19. Sipos G, Prasanna AN, Walter MC, O'Connor E, Bálint B, Krizsán K, Kiss B,
579 Hess J, Varga T, Slot J, Riley R, Bóka B, Rigling D, Barry K, Lee J, Mihaltcheva
580 S, LaButti K, Lipzen A, Waldron R, Moloney NM, Sperisen C, Kredics L,
581 Vágvölgyi C, Patrignani A, Fitzpatrick D, Nagy I, Doyle S, Anderson JB, Grigoriev
582 IV, Güldener U, Münsterkötter M, Nagy L. 2017. Genome expansion and lineage-
583 specific genetic innovations in the forest pathogenic fungi *Armillaria*. *Nat Ecol*
584 *Evol* **1**:1931–1941.
585 20. Dodd RB, Drickamer K. 2001. Lectin-like proteins in model organisms:
586 implications for evolution of carbohydrate-binding activity. *Glycobiology* **11**:71R–
587 79R.
588 21. Inbar J, Chet I. 1992. Biomimics of fungal cell-cell recognition by use of lectin-
589 coated nylon fibers. *J Bacteriol* **174**:1055–1059.
590 22. Inbar J, Chet I. 1996. The role of lectins in recognition and adhesion of the
591 mycoparasitic fungus *Trichoderma* spp. to its host. *Adv Exp Med Biol* **408**:229–
592 231.
593 23. Latgé JP, Kobayashi H, Debeaupuis JP, Diaquin M, Sarfati J, Wieruszeski JM,
594 Parra E, Bouchara JP, Fournet B. 1994. Chemical and immunological
595 characterization of the extracellular galactomannan of *Aspergillus fumigatus*.
596 *Infect Immun* **62**:5424–5433.

597 24. Wei SJ, Li GQ, Jiang DH, Wang DB. 2004. Effect of oxalic acid on spore
598 germination and mycelial growth of the mycoparasite *Coniothyrium minitans*.
599 *Acta Phytopathol Sin* **34**:199–203.
600 25. Ren L, Li GQ, Han YC, Jiang DH, Huang HC. 2007. Degradation of oxalic acid by
601 *Coniothyrium minitans* and its effects on production and activity of β-1,3-
602 glucanases of this mycoparasite. *Biol Control* **43**:1–11.
603 26. Ren L, Li GQ, Jiang DH. 2010. Characterization of some culture factors affecting
604 oxalate degradation by the mycoparasite *Coniothyrium minitans*. *J Appl Microbiol*
605 **108**:173–180.
606 27. Zeng L-M, Zhang J, Han Y-C, Yang L, Wu M-d, Jiang D-H, Chen W, Li G-Q.
607 2014. Degradation of oxalic acid by the mycoparasite *Coniothyrium minitans*
608 plays an important role in interacting with *Sclerotinia sclerotiorum*. *Environ*
609 *Microbiol* **16**:2591–2610.
610 28. Cessna SG, Sears VE, Dickman MB, Low PS. 2000. Oxalic acid, a pathogenicity
611 factor for *Sclerotinia sclerotiorum*, suppresses the oxidative burst of the host
612 plant. *Plant Cell* **12**:2191–2200.
613 29. Dumas MT, Boyonoski N, Jeng RS. 1989. Oxalic acid production by species of
614 *Armillaria* in the boreal mixedwood forest. In: Proc. 7th International Conference
615 on Root and Butt Rots. 9–16 Aug. 1988, Vernon and Victoria, British Columbia.
616 Forestry Canada, Pacific Forestry Centre, Victoria, B.C. 680 p. 593–601.
617 30. Munir E, Jun Yoon J, Tokimatsu T, Hattori T, Shimada M. 2001. A physiological
618 role for oxalic acid biosynthesis in the wood-rotting basidiomycete *Fomitopsis*
619 *palustris*. *Proc Natl Acad Sci U S A* **98**:11126–11130.

620 31. Wang Y, Wang Y. 2020. Oxalic acid metabolism contributes to full virulence and
621 pycnidial development in the poplar canker fungus *Cytospora chrysosperma*.
622 *Phytopathology* **110**:1319–1325.
623 32. Dubey M, Jensen DF, Karlsson M. 2015. The ABC transporter ABCG29 is
624 involved in H_2O_2 tolerance and biocontrol traits in the fungus *Clonostachys rosea*.
625 *Mol Genet Genom* **291**:677–686.
626 33. Ruocco M, Lanzuise S, Vinale F, Marra R, Turrà, Lois Woo S, Lorito M. 2009.
627 Identification of a new biocontrol gene in *Trichoderma* atroviride: the role of an
628 ABC transporter membrane pump in the interaction with different plant-
629 pathogenic fungi. *Mol Plant Microbe In* **22**:291–301.
630 34. Zhao H, Zhou T, Xie J, Cheng J, Chen T, Jiang D, Fu Y. 2020. Mycoparasitism
631 illuminated by genome and transcriptome sequencing of *Coniothyrium minitans*,
632 an important biocontrol fungus of the plant pathogen *Sclerotinia sclerotiorum*.
633 *Microb Genom* **6**:e000345.
634 35. Nygren K, Dubey M, Zapparata A, Iqbal M, Tzelepis GD, Brandström Durling M,
635 Funck Jensen D, Karlsson M. 2018. The mycoparasitic fungus *Clonostachys*
636 *rosea* responds with both common and specific gene expression during
637 interspecific interactions with fungal prey. *Evol Appl* **11**:931–949.
638 36. Atanasova L, Le Crom S, Gruber S, Coulpier F, Seidl-Seiboth V, Kubick CP,
639 Druzhinina IS. 2013. Comparative transcriptomics reveals different strategies of
640 *Trichoderma* mycoparasitism. *BMC Genom* **14**:121.
641 37. Cha JY, Igarashi T. 1996. Biological species of *Armillaria* and their mycoparasitic
642 associations with *Rhodophyllus abortivus* in Hokkaido. *Mycoscience* **37**:25–30.

643 38. Tregear JW, Roberts LM. 1992. The lectin gene family of *Ricinus communis*:
644 Cloning of a functional ricin gene and three lectin pseudogenes. *Plant Mol Biol*
645 **18**:515–525.
646 39. Pohleven J, Obermajer N, Sabotič J, Anžlovar S, Sepčić K, Kos J, Kralj B,
647 Štrukelj B, Brzin J. 2009. Purification, characterization and cloning of a ricin B-
648 like lectin from mushroom *Clitocybe nebularis* with antiproliferative activity
649 against human leukemic T cells. *Biochim Biophys Acta Gen Subj* **1790**:173–181.
650 40. Schubert M, Bleuler-Martinez S, Butschi A, Wälti MA, Egloff P, Stutz K, Yan S,
651 Wilson IBH, Hengartner MO, Aebi M, Allain FHT, Künzler M. 2012. Plasticity of
652 the β-trefoil protein fold in the recognition and control of invertebrate predators
653 and parasites by a fungal defence system. *PLoS Pathog* **8**:e1002706.
654 41. Žurga S, Pohleven J, Renko M, Bleuler-Martínez S, Sosnowski P, Turk D,
655 Künzler M, Kos J, Sabotič J. 2014. A novel beta-trefoil lectin from the parasol
656 mushroom (*Macrolepiota procera*) is nematotoxic. *FEBS J* **281**:3489–3506.
657 42. Bovi M, Cenci L, Perduca M, Capaldi S, Carrizo ME, Civiero L, Chiarelli LR,
658 Galliano M, Monaco HL. 2013. BEL beta-trefoil: a novel lectin with antineoplastic
659 properties in king bolete (*Boletus edulis*) mushrooms. *Glycobiology* **23**:578–592.
660 43. Sabotič J, Ohm RA, Künzler M. 2016. Entomotoxic and nematotoxic lectins and
661 protease inhibitors from fungal fruiting bodies. *Appl Microbiol Biotechnol* **100**:91–
662 111.
663 44. Pohleven J, Renko M, Magister S, Smith DF, Künzler M, Strukelj B, Turk D, Kos
664 J, Sabotič J. 2012. Bivalent carbohydrate binding is required for biological activity
665 of *Clitocybe nebularis* lectin (CNL), the N, N'-diacetyllactosediamine

666 (GalNAcbeta1-4GlcNAc, LacdiNAc)-specific lectin from basidiomycete *C.*
667 *nebularis*. *J Biol Chem* **287**:10602–10612.
668 45. Latgé JP. 2007. The cell wall: a carbohydrate armour for the fungal cell. *Mol*
669 *Microbiol* **66**:279–290.
670 46. de Man TJ, Stajich JE, Kubicek CP, Teiling C, Chenthamara K, Atanasova L,
671 Druzhinina IS, Levenkova N, Birnbaum SS, Barribeau SM, Bozick BA, Suen G,
672 Currie CR, Gerardo NM. 2016. Small genome of the fungus *Escovopsis weberi*, a
673 specialized disease agent of ant agriculture. *Proc Natl Acad Sci U S A* **113**:3567–
674 3572.
675 47. Kubicek CP, Herrera-Estrella A, Seidl-Seiboth V, Martinez DA, Druzhinina IS,
676 Thon M, Zeilinger S, Casas-Flores S, Horwitz BA, Mukherjee PK, Mukherjee M,
677 Kredics L, Alcaraz LD, Aerts A, Antal Z, Atanasova L, Cervantes-Badillo MG,
678 Challacombe J, Chertkov O, McCluskey K, Coulpier F, Deshpande N, von
679 Döhren H, Ebbole DJ, Esquivel-Naranjo EU, Fekete E, Flipphi M, Glaser F,
680 Gómez-Rodríguez EY. Gruber S, Han C, Henrissat B, Hermosa R, Hernández-
681 Oñate M, Karaffa L, Kosti I, Le Crom S, Lindquist E, Lucas S, Lübeck M, Lübeck
682 PS, Margeot A, Metz B, Misra M, Nevalainen H, Omann M, Packer N, Perrone G,
683 Uresti-Rivera EE, Salamov A, Schmoll M, Seiboth B, Shapiro H, Sukno S,
684 Tamayo-Ramos JA, Tisch D, Wiest A, Wilkinson HH, Zhang M, Coutinho PM,
685 Kenerley CM, Monte E, Baker SE, Grigoriev IV. 2011. Comparative genome
686 sequence analysis underscores mycoparasitism as the ancestral life style of
687 *Trichoderma*. *Genome Biol* **12**:R40.

688 48. Ihrmark K, Asmail N, Ubhayasekera W, Melin P, Stenlid J, Karlsson M. 2010.
689 Comparative molecular evolution of *Trichoderma* chitinases in response to
690 mycoparasitic interactions. *Evol Bioinform* **6**:1–26.
691 49. Xie BB, Qin QL, Shi M, Chen LL, Shu YL, Luo Y, Wang XW, Rong JC, Gong ZT,
692 Li D, Sun CY, Liu GM, Dong XW, Pang XH, Huang F, Liu W, Chen XL, Zhou BC,
693 Zhang YZ, Song ZY. 2014. Comparative genomics provides insights into
694 evolution of *Trichoderma* nutrition style. *Genome Biol Evol* **6**:379–390.
695 50. Han Y-C, Li G-Q, Yang L, Jiang D-H. 2011. Molecular cloning, characterization
696 and expression analysis of a *pacC* homolog in the mycoparasite *Coniothyrium*
697 *minitans. World J Microbiol Biotechnol* **27**:381–391.
698 51. Agerer R, Waller K. 1993. Mycorrhizae of *Entoloma saepium*: parasitism or
699 symbiosis? *Mycorrhiza* **3**:145–154.
700 52. Kobayashi H, Hatano K. 2001. A morphological study of the mycorrhiza of
701 *Entoloma clypeatum* f. *hybridum* on *Rosa multiflora*. *Mycoscience* **42**:83–90.
702 53. Shishikura M, Takemura Y, Sotome K, Maekawa N, Nakagiri A, Endo N. 2021.
703 Four mycelial strains of *Entoloma clypeatum* species complex form
704 ectomycorrhiza-like roots with *Pyrus betulifolia* seedlings in vitro, and one
705 develops fruiting bodies 2 months after inoculation. *Mycorrhiza* **31**:31–42.
706 54. Kohler A, Kuo A, Nagy LG, Morin E, Barry KW, Buscot F, Canbäck B, Choi C,
707 Cichocki N, Clum A, Colpaert J, Copeland A, Costa MD, Doré J, Floudas D, Gay
708 G, Girlanda M, Henrissat B, Herrmann S, Hess J, Högberg N, Johansson T,
709 Khouja H-R, LaButti K, Lahrmann U, Levasseur A, Lindquist EA, Lipzen A,
710 Marmeisse R, Martino E, Murat C, Ngan CY, Nehls U, Plett JM, Pringle A, Ohm

711 RA, Perotto S, Peter M, Riley R, Rineau F, Ruytinx J, Salamov A, Shah F, Sun
712 H, Tarkka M, Tritt A, Veneault-Fourrey C, Zuccaro A, Mycorrhizal Genomics
713 Initiative Consortium, Tunlid A, Grigoriev IV, Hibbett DS, Martin F. 2015.
714 Convergent losses of decay mechanisms and rapid turnover of symbiosis genes
715 in mycorrhizal mutualists. *Nat Genet* **47**:410–415.
716 55. Fukuda M, Nakashima E, Hayashi K, Nagasawa E. 2003. Identification of the
717 biological species of *Armillaria* associated with *Wynnea* and *Entoloma abortivum*
718 using PCR-RFLP analysis of the intergenic region (IGR) of ribosomal DNA.
719 *Mycol Res* **107**:1435–1441.
720 56. Schuierer S, Carbone W, Knehr J, Petitjean V, Fernandez A, Sultan M, Roma G.
721 2017. A comprehensive assessment of RNA-seq protocols for degraded and low-
722 quantity samples. *BMC Genom* **18**:1–13.
723 57. Crusoe MR, Alameldin HF, Awad S, Boucher E, Caldwell A, Cartwright R,
724 Charbonneau A, Constantinides B, Edvenson G, Fay S, Fenton J, Fenzl T, Fish
725 J, Garcia-Gutierrez L, Garland P, Gluck J, González I, Guermond S, Guo J,
726 Gupta A, Herr JR, Howe A, Hyer A, Härpfer A, Irber L, Kidd R, Lin D, Lippi J,
727 Mansour T, McA'Nulty P, McDonald E, Mizzi J, Murray KD, Nahum JR, Nanlohy
728 K, Nederbragt AJ, Ortiz-Zuazaga H, Ory J, Pell J, Pepe-Ranney C, Russ ZN,
729 Schwarz E, Scott C, Seaman J, Sievert S, Simpson J, Skennerton CT, Spencer
730 J, Srinivasan R, Standage D, Stapleton JA, Steinman SR, Stein J, Taylor B,
731 Trimble W, Wiencko HL, Wright M, Wyss B, Zhang Q, zyme e, Brown CT. 2015.
732 The khmer software package: enabling efficient nucleotide sequence analysis.
733 *F1000Res* **4**:900.

734 58. Grabherr MG, Haas BJ, Yassour M, Levin JZ, Thompson DA, Amit I, Adiconis X,
735 Fan L, Raychowdhury R, Zeng Q, Chen Z, Mauceli E, Hacohen N, Gnirke A,
736 Rhind N, di Palma F, Birren BW, Nusbaum C, Lindblad-Toh K, Friedman N,
737 Regev A. 2011. Trinity: reconstructing a full-length transcriptome without a
738 genome from RNA-Seq data. *Nat Biotechnol* **29**:644–652.
739 59. Mikheenko A, Prjibelski A, Saveliev V, Antipov D, Gurevich A. 2018. Versatile
740 genome assembly evaluation with QUAST-LG. *Bioinformatics* **34**:i142–i150.
741 60. Seppey M, Manni M, Zdobnov EM. 2019. BUSCO: Assessing genome assembly
742 and annotation completeness. In: Kollmar M (eds) Gene Prediction. Methods in
743 Molecular Biology, vol 1962. Humana, New York, NW.
744 61. Langmead B, Salzberg SL. 2012. Fast gapped-read alignment with Bowtie 2. *Nat*
745 *Methods* **9**:357–359.
746 62. Li B, Dewey CN. 2011. RSEM: accurate transcript quantification from RNA-Seq
747 data with or without a reference genome. *BMC Bioinform* **12**:323.
748 63. Robinson MD, McCarthy DJ, Smyth GK. 2010. edgeR: a Bioconductor package
749 for differential expression analysis of digital gene expression data. *Bioinformatics*
750 **26**:139–140.
751 64. Robinson MD, Oshlack A. 2010. A scaling normalization method for differential
752 expression analysis of RNA-seq data. *Genome Biol* **11**:R25.
753 65. Li H, Handsaker B, Wysoker A, Fennell T, Ruan J, Homer N, Marth G, Abecasis
754 G, Durbin R, 1000 Genome Project Data Processing Subgroup. 2009. The
755 Sequence Alignment/Map format and SAMtools. *Bioinformatics* **25**:2078–2079.

756 66. Bryant DM, Johnson K, DiTommaso T, Tickle T, Brian Couger M, Payzin-Dogru
757 D, Lee TJ, Leigh ND, Kuo T-H, Davis FG, Bateman J, Bryant S, Guzikowski AR,
758 Tsai SL, Coyne S, Ye WW, Freeman RM, Jr, Peshkin L, Tabin CJ, Regev A,
759 Haas BJ, Whited JL. 2017. A tissue-mapped azolotl de novo transcriptome
760 enables identification of limb regeneration factors. *Cell Rep* **18**:P762–P776.
761 67. Camacho C, Coulouris G, Avagyan V, Ma N, Papadopoulos J, Bealer K, Madden
762 TL. 2009. BLAST+: architecture and application. *BMC Bioinform* **10**:421.
763 68. Wheeler TJ, Eddy SR. 2013. nhmmer: DNA homology search with profile HMMs.
764 *Bioinformatics* **29**:3487–3489.
765 69. Finn RD, Bateman A, Clements J, Coggill P, Eberhardt RY, Eddy SR, Heger A,
766 Hetherington K, Holm L, Mistry J, Sonnhammer ELL, Tate J, Punta M. 2014.
767 Pfam: the protein families database. *Nucleic Acids Res* **42**:D222–D230.
768 70. Ashburner M, Ball CA, Blake JA, Botstein D, Butler H, Cherry JM, Davis AP,
769 Dolinski K, Dwight SS, Eppig JT, Harris MA, Hill DP, Issel-Tarver L, Kasarskis A,
770 Lewis S, Matese JC, Richardson JE, Ringwald M, Rubin GM, Sherlock G. 2000.
771 Gene Ontology: tool for the unification of biology. *Nat Genet* **25**:25–29.
772 71. Kanehisa M, Goto S. 2000. KEGG: Kyoto Encyclopedia of Genes and Genomes.
773 *Nucleic Acids Res* **28**:27–30.
774 72. Kanehisa M. 2019. Toward understanding the origin and evolution of cellular
775 organisms. *Protein Sci* **28**:1947–1951.
776 73. Kanehisa M, Furumichi M, Sato Y, Ishiguro-Watanabe M, Tanabe M. 2021.
777 KEGG: integrating viruses and cellular organisms. *Nucleic Acids Res* **49**:D545–
778 D551.

74. Zhang H, Yohe T, Huang L, Entwistle S, Wu P, Yang Z, Busk PK, Xu Y, Yin Y. 2018. dbCAN2: a meta server for automated carbohydrate-active enzyme annotation. *Nucleic Acids Res* **46**:W95–W101.

75. Miyauchi S, Kiss E, Kuo A, Drula E, Kohler A, Sánchez-García M, Morin E, Andreopoulos B, Barry KW, Bonito G, Buée M, Carver A, Chen C, Cichocki N, Clum A, Culley D, Crous PW, Fauchery L, Girlanda M, Hayes RD, Kéri Z, LaButti K, Lipzen A, Lombard V, Magnuson J, Maillard F, Murat C, Nolan M, Ohm RA, Pangilinan J, Pereira MF, Perotto S, Peter M, Pfister S, Riley R, Sitrit Y, Stielow JB, Szöllősi G, Žifčáková L, Štursová M, Spatafora JW, Tedersoo L, Vaario LM, Yamada A, Yan M, Wang P, Xu J, Bruns T, Baldrian P, Vilgalys R, Dunand C, Henrissat B, Grigoriev IV, Hibbett D, Nagy LG, Martin FM. 2020. Large-scale genome sequencing of mycorrhizal fungi provides insights into the early evolution of symbiotic traits. *Nat Commun* **11**:5125.

76. Steindorff AS, Carver A, Calhoun S, Stillman K, Liu H, Lipzen A, He G, Yan M, Pangilinan J, LaButti K, Ng V, Bruns TD, Grigoriev IV. 2020. Comparative genomics of pyrophilous fungi reveals a link between fire events and developmental genes. *Environ Microbiol* **23**:99–109.

77. Ruiz-Dueñas FJ, Barrasa JM, Sánchez-García M, Camarero S, Miyauchi S, Serrano A, Linde D, Babiker R, Drula E, Ayuso-Fernández I, Pacheco R, Padilla G, Ferreira P, Barriuso J, Kellner H, Castanera R, Alfaro M, Ramirez L, Pisabarro AG, Riley R, Kuo A, Andreopoulos W, LaButti K, Pangilinan J, Tritt A, Lipzen A, He G, Yan M, Ng V, Grigoriev IV, Cullen D, Martin F, Rosso MN, Henrissat B, Hibbett D, Martínez AT. 2020. Genomic analysis enlightens Agaricales lifestyle

802 evolution and increasing peroxidase diversity. *Mol Biol Evol*
803 doi:10.1093/molbev/msaa301.
804 78. Blin K, Shaw S, Steinke K, Villebro R, Ziemert N, Yup Lee S, Medema MH,
805 Weber T. 2019. antiSMASH 5.0: updates to the secondary metabolite genome
806 mining pipeline. *Nucleic Acids Res* **47**:W81–W87.
807 79. Collins C, Keane TM, Turner DJ, O'Keeffe G, Fitzpatrick DA, Doyle S. 2013.
808 Genomic and proteomic dissection of the ubiquitous plant pathogen, *Armillaria*
809 *mellea*: Toward a new infection model system. *J Proteome Res* **12**:2552–2570.
810 80. Floudas D, Held BW, Riley R, Nagy LG, Koehler G, Ransdell AS, Younus H,
811 Chow J, Chiniquy J, Lipzen A, Tritt A, Sun H, Haridas S, LaButtie K, Ohm RA,
812 Kües U, Blanchette RA, Grigoriev IV, Minto RE, Hibbett DS. 2015. Evolution of
813 novel wood decay mechanisms in Agaricales revealed by the genome
814 sequences of *Fistulina hepatica* and *Cylindrobasidium torrendii*. *Fungal Genet*
815 *Biol* **76**:78–92.
816 81. Koch RA, Yoon GM, Arayal UK, Lail K, Amirebrahimi M, LaButti K, Lipzen A,
817 Riley R, Barry K, Henrissat B, Grigoriev IV, Herr JR, Aime MC. Symbiotic
818 nitrogen fixation in the reproductive structures of a basidiomycete fungus. *Curr*
819 *Biol*, Accepted.
820 82. Katoh K, Standley DM. 2013. MAFFT multiple sequence alignment software
821 version 7: improvements in performance and usability. *Mol Biol Evol* **30**:772–780.
822 83. Castresana J. 2000. Selection of conserved blocks from multiple alignments for
823 their use in phylogenetic analysis. *Mol Biol Evol* **17**:540–552.

84. Kozlov AM, Darriba D, Flouri T, Morel B, Stamatakis A. 2019. RAxML-NG: a fast, scalable and user-friendly tool for maximum likelihood phylogenetic inference. *Bioinformatics* **35**:4453–4455.

85. Bengtsson-Palme J, Ryberg M, Hartmann M, Branco S, Wang Z, Godhe A, De Wit P, Sánchez-García M, Ebersberger I, de Sousa F, Amend A, Jumpponen A, Unterseher M, Kristiansson E, Abarenkov K, Bertrand YJK, Sanli K, Eriksson KM, Vik U, Veldre V, Nilsson RH. 2013. Improved software detection and extraction of ITS1 and ITS2 from ribosomal ITS sequences of fungi and other eukaryotes for analysis of environmental sequencing data. *Methods Ecol Evol* **4**:914–919.

86. Guo T, Wang HC, Xue WQ, Zhao J, Yang ZL. 2016. Phylogenetic analyses of *Armillaria* reveal at least 15 phylogenetic lineages in China, seven of which are associated with cultivated *Gastrodia elata*. *PLoS One* **11**:e0154794.

87. Coetzee MPA, Wingfield BD, Harrington TC, Dalevi D, Coutinho TA, Wingfield MJ. 2000. Geographical diversity of *Armillaria mellea* s. s. based on phylogenetic analysis. *Mycologia* **92**:105–113.

88. Coetzee MPA, Wingfield BD, Bloomer P, Wingfield MJ. 2005. Phylogenetic analyses of DNA sequences reveal species partitions amongst isolates of *Armillaria* from Africa. *Mycol Res* **109**:1223–1234.

89. Schneider-Maunoury L, Deveau A, Moreno M, Todesco F, Belmondo S, Murat C, Courty P-E, Jąkalski M, Selosse M-A. 2020. Two ectomycorrhizal truffles, *Tuber melanosporum* and *T. aestivum*, endophytically colonise roots of non-ectomycorrhizal plants in natural environments. *New Phytol* **225**:2542–2556.

90. Coetzee MPA, Bloomer P, Wingfield MJ, Wingfield BD. 2011. Paleogene radiation of a plant pathogenic mushroom. *PLoS One* **6**:e28545.

91. Osmundson TW, Robert VA, Schoch CL, Baker LJ, Smith A, Robich G, Mizzan L, Garbelotto MM. 2013. Filling gaps in biodiversity knowledge for macrofungi: contributions and assessment of an herbarium collection DNA barcode sequencing project. *PLoS One* **8**:e62419.

92. Kasper-Pakosz R, Pietras M, Łuczaj Ł. 2016. Wild and native plants and mushrooms sold in the open-air markets of south-eastern Poland. *J Ethnobiol Ethnomed* **12**:45.

93. Hughes KW, Petersen RH, Lodge DJ, Bergemann SE, Baumgartner K, Tulloss RE, Lickey E, Cifuentes J. 2013. Evolutionary consequences of putative intra- and interspecific hybridization in agaric fungi. *Mycologia* **105**:1577–1594.

94. Potyralska A, Schmidt O, Moreth U, Łakomy P, Siwecki R. 2002. rDNA-ITS sequence of *Armillaria* species and a specific primer for *A. mellea*. *For Genet* **9**:119–124.

95. Ortega A, Moreno G, Platas G, Pelaez F. 2008. A new *Armillaria mellea* variant from tops of coastal sand dunes in southern Spain. *Mycotaxon* **104**:349–364.

96. Vu D, Groenewald M, de Vries M, Gehrmann T, Stielow B, Eberhardt U, Al-Hatmi A, Groenewald JZ, Cardinali G, Houbraken J, Boekhout T, Crous PW, Robert V, Verkley GJM. 2019. Large-scale generation and analysis of filamentous fungal DNA barcodes boosts coverage for kingdom fungi and reveals thresholds for fungal species and higher taxon delimitation. *Stud Mycol* **92**:135–154.

97. Binder M, Hibbett DS, Wang Z, Farnham WF. 2006. Evolutionary relationships of *Mycaureola dilseae* (Agaricales), a basidiomycete pathogen of a subtidal rhodophyte. *Am J Bot* **93**:547–556.

98. Haelewaters D, Dirks AC, Kappler LA, Mitchell JK, Quijada L, Vandegrift R, Buyck B, Pfister DH. 2018. A preliminary checklist of fungi at the Boston Harbor Islands. *Northeast Nat* **25**:45–76.

99. Kim M-S, Klopfenstein NB, Hanna JW, McDonald GI. 2006. Characterization of North American *Armillaria* species: genetic relationships determined by ribosomal DNA sequences and AFLP markers. *For Path* **36**:145–164.

100. Schnabel G, Ash JS, Bryson PK. 2005. Identification and characterization of *Armillaria tabescens* from the southeastern United States. *Mycol Res* **109**:1208–1222.

892 TABLE 1 Ten most highly expressed *E. abortivum* genes in sporocarps and carpophoroids

Gene	Annotation	Cond.	C (TMM)	S (TMM)	logFC	*q*-value
ENT_DN2762_c0_g3	Oxalate decarboxylase	C	68,724	238	-8.5	4.5×10^{-317}
ENT_DN1212_c0_g1	Hypothetical protein	C/S	55,939	12,590	-2.5	4.3×10^{-49}
ENT_DN3063_c0_g2	Oxalate decarboxylase	C	48,157	135	-8.8	0
ENT_DN1952_c0_g2	Acid phosphatase	C	19,999	677	-5.2	1.3×10^{-169}
ENT_DN4045_c1_g1	Hypothetical protein	C	19,965	3,374	-2.9	3.4×10^{-63}
ENT_DN5742_c0_g1	Hypothetical protein	C	11,229	23	-9.3	6.9×10^{-220}
ENT_DN4332_c0_g1	Hypothetical protein	C	11,038	607	-4.5	4.7×10^{-77}
ENT_DN1952_c0_g1	Acid phosphatase	C	10,766	673	-4.4	1.9×10^{-122}
ENT_DN2936_c0_g2	Hypothetical protein	C	9,212	3,686	NS	
ENT_DN3086_c0_g1	Hypothetical protein	C	9,076	1,563	-2.9	2.2×10^{-62}
ENT_DN1375_c0_g1	Trehalase	S	1,934	17,890	2.9	6.5×10^{-37}
ENT_DN5247_c0_g3	Hypothetical protein	S	2,718	7,204	NS	
ENT_DN761_c0_g2	Hypothetical protein	S	7,405	6,918	NS	
ENT_DN521_c0_g2	Hypothetical protein	S	6,045	6,424	NS	
ENT_DN852_c0_g1	Hypothetical protein	S	123	5,429	5.1	2.0×10^{-142}
ENT_DN3621_c0_g2	RNA polymerase	S	1,977	5,138	NS	
ENT_DN6707_c0_g1	Hypothetical protein	S	1,654	5,027	NS	
ENT_DN2379_c0_g1	TPR-like protein	S	4,862	5,017	NS	
ENT_DN466_c0_g1	Auxin efflux carrier	S	1,205	4,333	NS	

913 Cond.: condition in which each gene was most highly expressed, referring to either the carpophoroids (C) or sporocarps (S). NS: not
914 significantly differentially expressed in either condition. Negative logFC values are significantly differentially upregulated in the carpophoroid,
915 whereas positive values are significantly differentially upregulated in the sporocarp. Transcripts discussed in the text include two oxalate
916 decarboxylases (ENT_DN2762_c0_g3, ENT_DN3063_c0_g2), three β-trefoil-type lectins (ENT_DN4359_c0_g1, ENT_DN1877_c0_g1,
917 ENT_DN4255_c0_g1), three ABC transporters (ENT_DN1537_c0_g1, ENT_DN189_c0_g1, ENT_DN3860_c0_G1), two chitinases
918 (ENT_DN2096_c0_g1, ENG_DN4507_c0_g3) and 14 MFS transcripts (ENT_DN409_c0_g1, ENT_DN1954_c0_g1, ENT_DN1998_c0_g1,
919 ENT_DN2070_c0_g1, ENT_DN2744_c0_g1, ENT_DN3292_c0_g1, ENT_DN3474_c0_g1, ENT_DN3861_c0_g1, ENT_DN3943_c0_g1,
920 ENT_DN3943_c0_g2, ENT_DN3981_c0_g1, ENT_DN4751_c0_g2, ENT_DN6588_c0_g1, ENT_DN6695_c0_g1).

921 TABLE 2 Ten most highly expressed *Armillaria* genes in sporocarps and carpophoroids

Gene	Annotation	Cond.	C (TMM)	S (TMM)	logFC	*q*-value
ARM_DN1755_c2_g1	Cell wall galactomannoprotein	S	0	36,479	13.5	4.0×10^{-182}
ARM_DN3840_c0_g1	Serine carboxypeptidase	S	12	29,472	6.7	7.9×10^{-100}
ARM_DN22943_c1_g1	Rab geranylgeranyltransferase	S	21	18,649	5.1	3.8×10^{-89}
ARM_DN1737_c0_g1	LysM-domain-containing protein	S	0	14,557	15.9	3.0×10^{-159}
ARM_DN1699_c3_g1	Hypothetical protein	S	9	12,848	5.8	1.6×10^{-94}
ARM_DN1314_c0_g1	Chondroitin AC/alginate lyase	S	102	11,436	2.2	3.7×10^{-25}
ARM_DN20980_c0_g1	Glycopeptide	S	0	10,449	15.4	3.4×10^{-139}
ARM_DN8135_c0_g1	Rasp f 7 allergen	S	0	9,014	11.5	1.8×10^{-58}
ARM_DN4971_c0_g2	Aldehyde dehydrogenase	S	103	8,688	NS	
ARM_DN1205_c0_g1	Hypothetical protein	S/C	9,049	8,348	-4.8	2.1×10^{-74}
ARM_DN5170_c0_g1	Hypothetical protein	C	2,086	377	-7.1	6.9×10^{-150}
ARM_DN23207_c0_g2	Senescence-associated	C	1,711	2,482	-4.1	6.6×10^{-61}
ARM_DN996_c0_g1	Senescence-associated	C	1,423	1,090	-5.0	3.0×10^{-73}
ARM_DN409_c1_g1	Elongation factor 1-alpha	C	769	1,154	-4.1	4.0×10^{-155}
ARM_DN1893_c0_g1	Hypothetical protein	C	722	58	-8.3	5.3×10^{-109}
ARM_DN693_c0_g1	Hypothetical protein	C	520	840	-3.9	1.1×10^{-48}
ARM_DN1222_c0_g1	CYS3-cystathionine gamma-lyase	C	485	717	-4.1	5.5×10^{-27}
ARM_DN1146_c0_g4	Heat shock protein 70	C	431	2,361	-2.2	1.7×10^{-54}
ARM_DN3800_c0_g1	ATP synthase F1	C	300	4,686	NS	

942 Cond.: condition in which each gene was most highly expressed, referring to either the carpophoroids (C) or sporocarps (S).
943 NS: not significantly differentially expressed in either condition. Negative logFC values are significantly differentially
944 upregulated in the carpophoroid, whereas positive values are significantly differentially upregulated in the sporocarp.
945 Transcripts discussed in the text were an isocitrate lyase (ARM_DN1_c7_g1), two putative senescence-associated proteins
946 (ARM_DN23207_c0_g2, ARM_DN996_c0_g1), and a heat shock protein (ARM_DN1146_c0_g4).

FIG 1 The components of this fungal interaction in nature. (A) *Armillaria* sporocarps. (B) *Entoloma abortivum* sporocarps; photo taken by Eva Skific. (C) Carpophoroids. (D) A group of *E. abortivum* sporocarps and carpophoroids, with the carpophoroids indicated by arrows; photo taken by Andrew Loyd. Scale bars in A–C are equal to 1 cm and in D are equal to 10 cm.

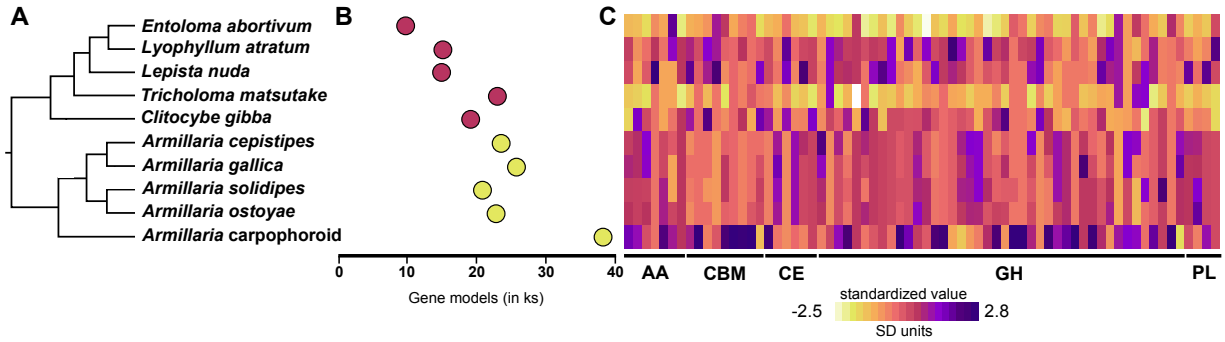

FIG 2 Number of total gene models and gene copy numbers of CAZymes. (A) A representative phylogeny is a representation based off phylogenetic evidence from Sipos et al. (2017) and Dentinger et al. (2016). (B) Number of gene models in the transcriptome of the *Armillaria* and *E. abortivum* generated in this study, along with those of closely related species from previously generated genomic data. (C) Heat map showing gene copy numbers of plant cell wall degrading enzymes detected in the transcriptomes of *E. abortivum* and *Armillaria*, along with other closely related species. Abbreviations: AA: Auxiliary Activities; CBM: Carbohydrate-Binding Modules; CE: Carbohydrate Esterase; GH: Glycoside Hydrolase; PL: Polysaccharide Lyase.

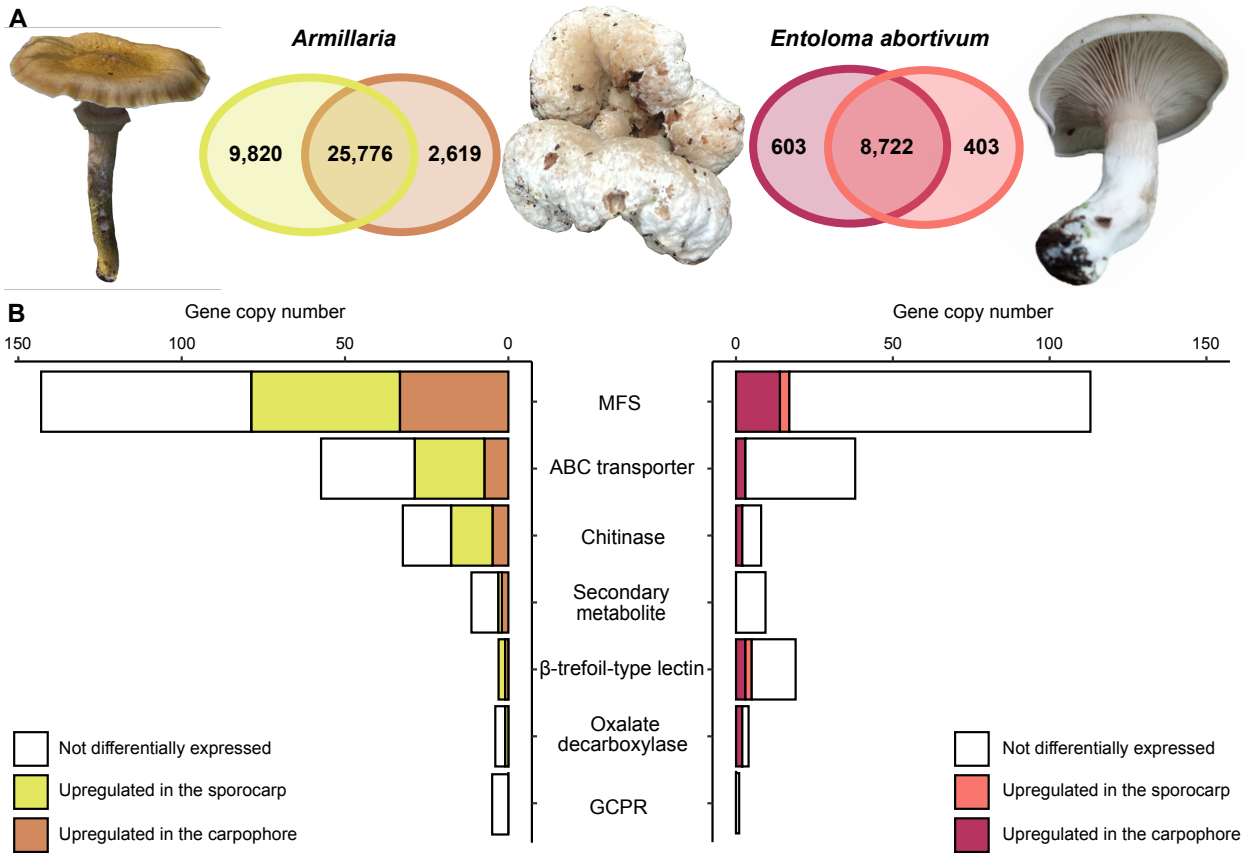

FIG 3 Differentially expressed genes in the sporocarp and carpophoroid. (A) Venn diagram showing the number of differentially expressed genes between the sporocarp and carpophoroid in *Armillaria* and *E. abortivum*; photo of *E. abortivum* taken by Eva Skific. (B) Bar graph showing the number of gene copies of genes important in mycoparasitic interactions. The white portion of the bar shows the number of these genes detected in the transcriptome but not differentially expressed, while the darker colors (brown and purple, respectively) show the number of these genes that are significantly upregulated by each species in the carpophoroid and the lighter colors (yellow and coral, respectively) show the number of these genes that are significantly upregulated by each species in their respective sporocarp.

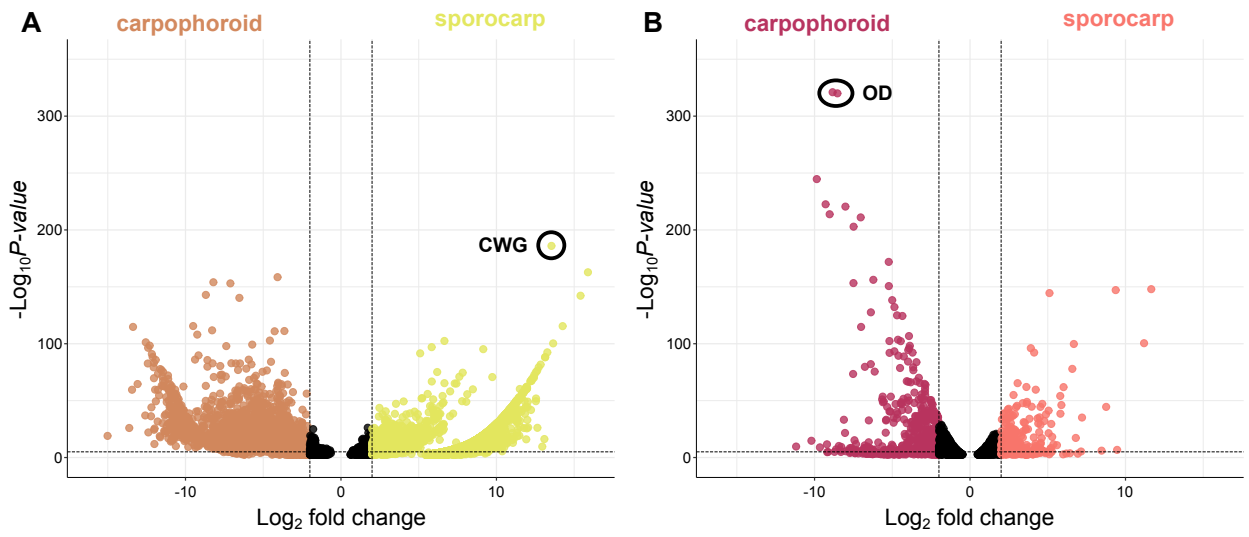

975

976 **FIG 4** Volcano plots. Each dot represents a gene plotted according to its logFC and the

977 -log10 of its *p*-value. All genes with a *q*-value < 0.05 are shown. Black dots represent a

978 gene with a non-significant logFC (-2 < logFC < 2). (A) *Armillaria*. (B) *E. abortivum*. Dots

979 with a black circle around them are annotated according to the abbreviations OD:

980 oxalate decarboxylase; CWG: cell wall galactomannoprotein.

981

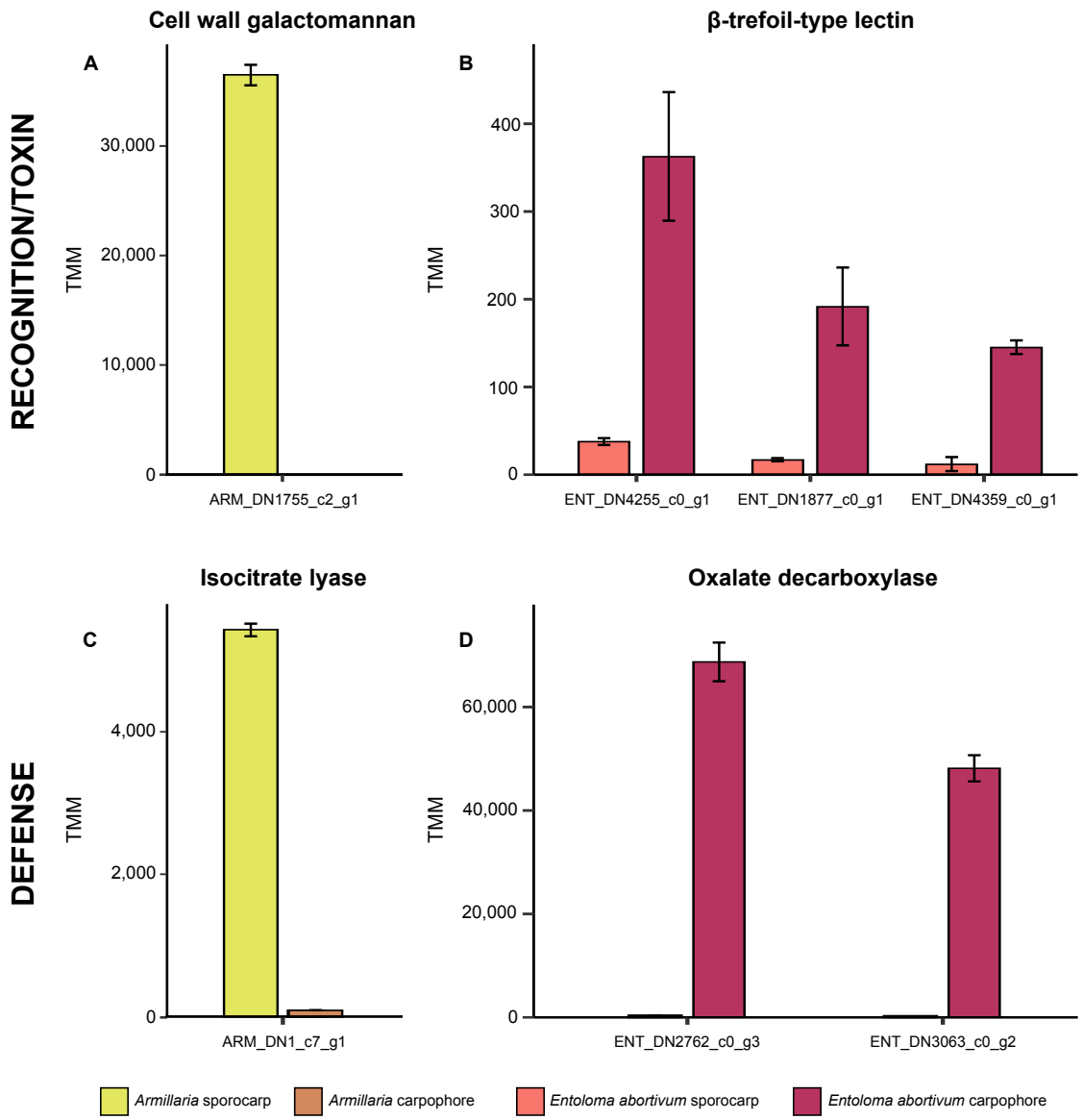

FIG 5 Genes in both *Armillaria* and *E. abortivum* that are putatively important in the recognition and defense responses during this mycoparasitic interaction. (A) One *Armillaria* cell wall galactomannan that is significantly upregulated in the sporocarp; (B) three *E. abortivum* β-trefoil-type lectins that are significantly upregulated in the carpophoroid; (C) one *Armillaria* gene that codes for isocitrate lyase that is significantly upregulated in their sporocarps; and (D) two *E. abortivum* genes that code for oxalate

989 decarboxylases that are significantly upregulated in the carpophoroids. All results are

990 shown as means ± standard error of the mean.

991

992

993

994

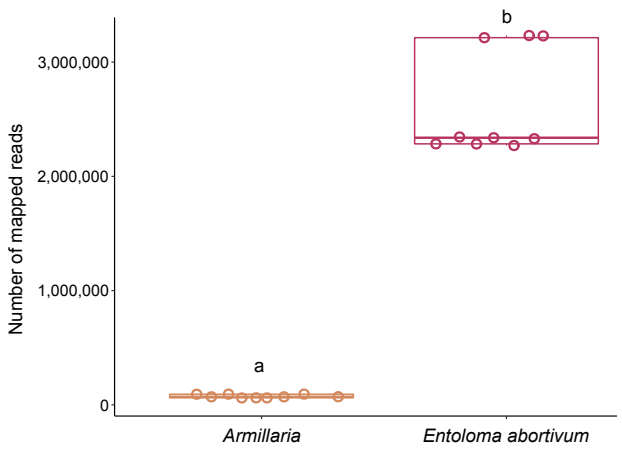

FIG 6 Boxplots of number of carpophoroid reads that mapped to *Armillaria* and *E. abortivum* when MAPQ = 30. Individual data points are indicated for each species with an open circle. The continuous line within each box represents the mean number of mapped reads. Species labeled with different letters (a to b) have a statistically significant ($p < 0.05$) different number of mapped reads in the carpophoroid.

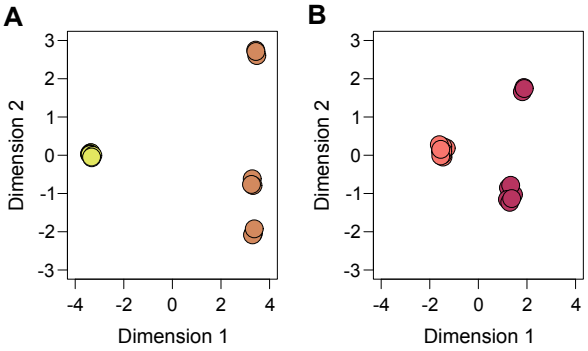

1004

1005 **FIG 7** Multidimensional scaling plot of distances between gene expression profiles for

1006 each sample. (A) *Armillaria* sporocarps and carpophoroids. (B) *E. abortivum* sporocarps

1007 and carpophoroids. For both figures, the lighter colors on the left represent the

1008 sporocarps, while the darker colors on the right represent the carpophoroids.

1009

A
Armillaria ostoyae
Armillaria solidipes
Armillaria cepistipes
Armillaria gallica
Armillaria mellea
USA: Michigan JRH 2446
Guyanagaster necrorhizus
Cylindrobasidium torrendii
B
Western North America
USA: California AF163597
USA: California FJ664596
USA: California FJ664595
USA: California AF163596
USA: California AF163595
USA FJ664593
USA: South Carolina AY526604
USA: South Carolina AY526602
USA: New Hampshire KT822256
USA: Georgia MG931920
USA: Virgina AY213584
USA: Virgina AY213585
USA: South Carolina AY526603
USA: South Carolina MG931929
USA: Minnesota MG931908
USA: Wisconsin AY213586
USA: Massachusetts AY789081
USA: Michigan JRH 2446
USA: New Hampshire AY213587
USA: New Hampshire AF163587
Eastern North America
USA: Massachusetts MF161188
USA: New Hampshire AF163588
USA: Tennessee MF755264
USA: Massachusetts AF163589
USA: Massachusetts AF163590
Scotland JF313749
Italy KP960556
Italy KP960538
Poland KX756392
Italy KP960550
Italy KP960558
Portugal KP960535
United Kingdom KX618581
Hungary AF163581
Italy CRA PAC2824
United Kingdom MH855148
United Kingdom KX618568
United Kingdom AF163582
United Kingdom AF163578
France MG931767
United Kingdom AF163579
Italy KP960563
France HQ232290
Italy KP960555
Iran AF163583
Ukraine JN657466
United Kingdom KX618569
Italy KP960539
Denmark MG931762
Italy KP960554
France MN660639
Italy KP960552
Slovenia KF020706
France JN657464
Poland AY848938
France AF163584
France JN657465
France AF163586
Italy FJ875692
Italy KP960564
Spain EU266545
France AF163585
Italy KP960536
Slovenia AJ250051
Sweden KY352514
United Kingdom AF163580
Italy JF907776
Italy KP960537
Italy KP960561
Italy KP960565
Italy KP960562
Italy KP960566
Europe
Japan MF095794
Spain EU266546
Italy KP960557
Azerbaijan B1458
South Korea AF163591
Japan AF163594
South Korea AF163592
South Korea AF163593
China KF032535
China KF032532
China KF032530
China KF032534
Japan KT822246
China: Sichuan KT822245
Tunisia KU863550
China: Yunnan KT822249
China KF032536
Asia
China: Zhejiang KT822254
Tibet MG931786
China: Hubei HKAS86591
China: Zhejiang KT822244
China: Yunnan MG931746
China: Lijang KP162319
China: Yunnan MG931782
China KJ643339
China: Yunnan KT822255
China: Yunnan KT822242
China: Yunnan KT822243
China: Ghizhou KT822253
China: Yunnan KT822251
Armillaria gemina IIJB 38A
Armillaria sinapina V48.5.1
Armillaria puiggarii MCA 3111
Armillaria luteobubalina VM5.2
0.03

1010

1011 **FIG 8** Phylogenetic placement of the *Armillaria* species used in this analysis. (A)
1012 Maximum likelihood phylogeny of *Armillaria* species and *Guyanagaster necrorhizus*
1013 generated from the analysis of 100 random BUSCOs. The outgroup taxon is
1014 *Cylindrobasidium torrendii*. Each node is fully supported with 100% bootstrap
1015 supported. (B) Maximum likelihood phylogeny of *Armillaria mellea* phylogenetic tree
1016 generated from the analysis of the ITS region. Branches with 70% or more bootstrap
1017 support are thickened. Outgroup taxa include *A. gemina, A. luteobubalina*, *A. puiggarii*
1018 and *A. sinapina*. The *Armillaria* specimen analyzed during this study is in bold and
1019 yellow in both phylogenies.
1020
1021